NONEQUILIBRIUM REENTRY

A.S. Filatyev and O.V. Yanova.

Central Aerohydrodynamic Institute (TsAGI)
Zhukovsky, 140160 Moscow Region, RUSSIA

Abstract

The basic theoretical results for the problem of minimizing loads in the nonequilibrium atmospheric reentry with subcircular velocities are generalized. For the class of initial conditions under consideration, descent vehicles fail to attain the quasistationary gliding regime prior to the moment of passing peak loads which, as a result, can reach excessive values. Similar regimes are realized in returning spent components of space transport systems, during test suborbital flights and in the case of emergence orbiter recovery after ascent abortion.

The investigation is based on direct matching analytical solutions for the state and adjoint equations in characteristic regions with negligible and dominant influence of aerodynamic forces.

The analysis is given to the structure of the optimal aerodynamic and thrust control, as well as the effectiveness depending on the vehicle parameters and initial conditions. It is proved that the optimal control structure changes when the velocity at the reentry trajectory apogee reaches a critical value $V_{crit.}$. The physical meaning $V_{crit.}$ is that it is the initial velocity at which the reentry loads are extreme. The critical velocity is estimated analytically. It is proved that the critical, in terms of maximum overload, velocity rises as the L/D-ratio decreases not exceeding $1/\sqrt{2}$ of the local circular velocity. At $L/D>1.8$, the critical velocity degenerates, because the reentry overload decreases monotonically with initial velocity increase. A high accuracy of coinciding these estimates with the numerical integration of the equations of motion is shown.

Some examples of practical applications of the results obtained are indicated.

1. Introduction

In returning spent components of space transport systems, during test suborbital flights, recovering reentry vehicles after orbital ascent abort and in other similar cases, the atmospheric reentry occurs at velocities which are smaller than the local circular velocity.

The practical experience in operating with space rocket vehicles and the results of theoretical investigations testify that the atmospheric reentry at subcircular velocities can result in loads acting on the vehicle and its components which exceed many times (occasionally by orders of magnitude) loads characteristic of descent from orbit.

For example, occasions are known that spent boosters did not stand the atmospheric reentry loads. As a result of the failure, booster's parts were scattered over the area exceeding the alienation zone.

On April 5, 1975, when the space vehicle "Soyuz-18-1" was inserted into the orbit, the third-stage engine failed to start. Following the emergence separation from the launcher, the vehicle performed a suborbital flight to land safely. However, while entering the dense atmospheric the cosmonauts V. Lazarev and O. Makarov had to endure overloads exceeding 20g.

The analysis of possible aftereffects due to orbital insertion abort which was carried out at earlier stages of designing the aerospace aircraft "Buran" reveals that after the emergency separation from the second stage the dynamic pressures during the atmospheric reentry can exceed the admissible limit several tens times.

The problem of reducing loads during the nonequilibrium reentry of vehicles at subcircular velocities was considered in earlier publications of the author [1-3] (first two articles are published only in Russian). Among the publications of other authors, the works [4-7] should first of all be noted. The integrals of state and adjoint systems, as well as the laws of optimal control of a rather general form which are contained in these articles may be used, in particular, to study the problem of minimizing loads for suborbital trajectories. The analytical solutions [2, 3, 6-9] are based on the method of matching the solutions of equations for Keplerian motion for the initial flight arc and equations of Allen-Eggers [10] for the flight section in the dense atmospheric layers. The existence of the adjoint system integrals for Keplerian trajectories was first shown in [11].

The advantage of the analytical solutions lies in the capability of performing a qualitative analysis and a quantitative assessment of the influence of the system parameters and disturbances on the functional rather than in the derivation of formulas for a "fast" prediction of the functional in terms of a current state vector (as for real flight conditions, the application of the exact formulas often proves to be a more complicated approach than a numerical integration of the equations of motion).

The present article employs approximate analytical zero-order [5] solutions which yield accurate assessments of the functional and describe properly the behavior of the

influence functions (adjoint variables) on the reentry trajectory. By applying the Bli. , formula [12] to assess variations in the functional for varying right-hand sides of the equations of motion and varying parameters of the control and the state vector it is possible both to investigate qualitatively the optimal control structure and to estimate quantitatively the influence of these factors on the functional with an adequate accuracy. In particular, the article contains some analytical estimates of the effectiveness of reducing maximum loads during the atmospheric reentry by using aerodynamic control, thrust and variations in the initial conditions. Besides, the influence of assumptions, used in the mathematical model, on the functional are evaluated which make it possible to adjust the model parameters according to real flight conditions and which can be applied to increase the accuracy of predicting the functional in terms of local state vector.

The effectiveness of applying the analytical relations is confirmed by exact numerical solutions of the state and adjoint equations in a wide range of parameters. The calculations are performed using the program package "ASTER" for indirect trajectory optimization [13].

Some applications of the obtained analytical results to solve practical problems are indicated.

2. Problem statement

The dimensionless equations for the vehicle center of mass in the vertical plane over the spherical nonrotating Earth are as follows:

$$\begin{aligned}
&\dot v = \left(-\mu\rho v^2 + P\cos\varphi\right)/m - \sin\gamma/R^2 \equiv F_v \\
&\dot\gamma = \left(\mu K\rho v^2 + P\sin\varphi\right)/(mv) + \\
&\quad + \left(1 - \frac{1}{v^2 R}\right)\frac{v\cos\gamma}{R} \equiv F_\gamma \qquad (1)\\
&\dot h = v\sin\gamma \equiv F_h \\
&\dot m = -\frac{P}{c} \equiv F_m,
\end{aligned}$$

where $(\dot{})$ means differentiation with respect to time t, $t\in[t_i,t_f]$, v is the velocity, γ is the flight path angle, h is the altitude, m is the mass, ρ is the density of the atmosphere, for the exponential atmosphere model $\rho=e^{-\beta h}$, $\beta=const\approx 900$, P is the thrust-to-weight ratio; φ is the thrust angle-of-attack; c is the velocity of gases issuing engine nozzles; $\mu = a_r c_D$, $K = c_L/c_D$, c_L, c_D are the aerodynamic effective lift and drag coefficients, $a_r = \rho_E R_E F/(2m_i)$ is the dimensialization parameter, R_E is the Earth's radius, ρ_E is the atmosphere density at sea level; F is the reference area, m_i is the initial mass.

Let us consider a general-form functional to be minimized:

$$\Phi = q_{\max} = \max_t q \Rightarrow \min, \qquad (2)$$

where $q = \rho^{K_h} v^{K_v}$. (3)

The function q is in proportion to the dynamic pressure when

$$K_h = 1,\ K_v = 2 \qquad (4)$$

and to the heating rate at [4,5]

$$K_h = 0.5;\ 3 \le K_v \le 3.5\ . \qquad (5)$$

In what follows, convective heating rate will be estimated under assumption that[14]

$$K_h = 0.5;\ K_v = 3.25\ . \qquad (6)$$

Let us assume that a flight starts at velocities v_i which are smaller than the local circular velocity $v_c = \frac{1}{\sqrt{R}}$:

$$v_i\sqrt{R_i} < 1, \qquad (7)$$

and at sufficiently great altitudes where the gravitational forces are considerably in excess of the aerodynamic forces:

$$n_i = \mu\sqrt{1+K^2}\,\rho_i v_i^2 \ll n_* \approx 1. \qquad (8)$$

Unless otherwise specified, we shall consider only a coasting flight:

$$P = 0. \qquad (9)$$

Let a problem be stated to find an optimal control by using the aerodynamic drag coefficient

$$c_{D\min} \le c_D \le c_{D\max}, \qquad (10)$$

the effective aerodynamic lift coefficient

$$c_{L\min} \le c_L \le c_{L\max} \qquad (11)$$

and the thrust vector of the propulsion system with a relatively small characteristic velocity margin ΔV_{char} when the thrust action may be considered as a small disturbance of the coasting flight [1]. Also, we shall determine an optimal arrangement of the reentry trajectory portions, where the application of the above-outlined controls ensures a maximum reduction in the functional, and shall estimate qualitatively the effectiveness of optimal control actions δu using sensitivity functions $\frac{\partial\Phi}{\partial u}$.

In order to solve the stated problem we shall introduce adjoint equations

$$\frac{d\Psi}{dt} = -\frac{\partial F^{\mathsf T}}{\partial x}\cdot\Psi, \qquad (12)$$

where $x=\{v,\gamma,h,m\}$ is the state vector and $F = x$, $\Psi = \{\Psi_v,\Psi_\gamma,\Psi_h,\Psi_m\}$ is the adjoint vector.

Let at the point of attaining a maximum q(t):

$$t = t_f:\ \frac{dq}{dt} = \left(-K_h\beta F_h + \frac{K_v F_v}{v}\right)q = 0, \qquad (13)$$

the transversality condition be imposed in the form

$$\Psi(t_f)=\left(\frac{\partial q}{\partial x}\right)^{\mathrm{T}}=\left\{\frac{K_v q}{v},0,-\beta K_h q,0\right\}. \tag{14}$$

Then, in accordance with the Bliss's formula [12], the solution of set (12) and (14) simultaneously with set (1) and (13) yields the functions of the influence of current state vector variations on the functional (2) and (3):

$$\Psi(t)\equiv\frac{\partial q_{\max}}{\partial x(t)}. \tag{15}$$

In accordance with the maximum principle[15] for the set (1), the functional (2), (3) and the transversality conditions (14), the optimal control is governed by the following relations

$$\begin{aligned}
c_{D\mathrm{opt}}&=\begin{cases}c_{D\max}, & \Psi_v>0,\\ c_{D\min}, & \Psi_v<0,\end{cases}\\
c_{L\mathrm{opt}}&=\begin{cases}c_{L\max}, & \Psi_\gamma>0,\\ c_{L\min}, & \Psi_\gamma<0,\end{cases}\\
\sin\varphi_{\mathrm{opt}}&=-\frac{\Psi_\gamma}{\sqrt{(v\Psi_v)^2+\Psi_\gamma^2}};\ \cos\varphi_{\mathrm{opt}}=-\frac{\Psi_v v}{\sqrt{(v\Psi_v)^2+\Psi_\gamma^2}}
\end{aligned} \tag{16}$$

If variations in c_D and c_L are limited by the equality $c_D = c_D(c_L)$, then

$$\left\{c_{D\mathrm{opt}},c_{L\mathrm{opt}}\right\}:\ \frac{dc_D}{dc_L}=\frac{\Psi_\gamma}{\Psi_v v},\ \ \Psi_v\frac{d^2c_D}{dc_L^2}<0.$$

3. Approximate analytical solution

It is obvious that the problem of reducing loads during the atmospheric reentry is actual only when these loads are great

$$n_f=\left[\mu\sqrt{1+K^2}\rho v^2\right]_{t_f}\gg 1. \tag{17}$$

Thus, the reentry vehicle passes successively two regions: the "upper" region where the aerodynamic forces are small (see condition (8)) and the "lower" one where the aerodynamic forces dominate over the gravitational and inertial forces (see (17)).

For the analytical solution to be obtained let us assume [6] that the trajectory is obtained by matching two sections. In the upper region, the aerodynamic forces in (1) can be neglected and the vehicle moves along the arc of an ellipse in accordance with the Kepler's laws. In the lower region, the aerodynamic forces dominate, on the contrary, while the gravitational and inertial terms in (1) can be neglected (hypothesis of Allen-Eggers [10]). From here on, the variables in the upper region will be denoted, if necessary, with superscript (-), and in the lower region with (+).

The regions will be matched at a certain conditional altitude h_* of the upper boundary of the dense atmospheric layers (Fig. 1)

$$h_*:\ \ \mu\sqrt{1+K^2}\rho v^2=n_*\approx 1, \tag{18}$$

provided the state vector is continuous

$$x_*^-=x_*^+\ . \tag{19}$$

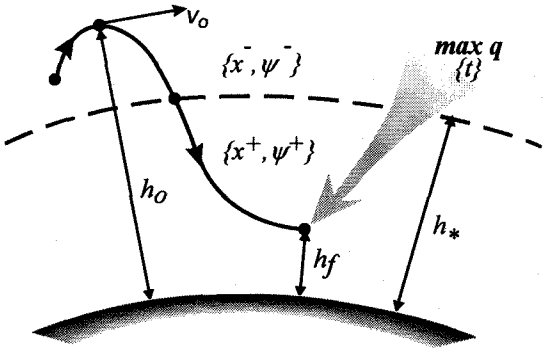

Fig. 1. Nonequilibrium reentry trajectory.

Suppose that

$$c_D\equiv\mathrm{const},\quad c_L\equiv\mathrm{const},\quad \beta\equiv\mathrm{const}. \tag{20}$$

Under above-outlined assumptions made in the set of equations (1), (12) and (14) we have the following first integrals:

"Upper" region

$$\begin{aligned}
v^-&=v_0\sqrt{1+\frac{2\Delta\bar h}{u_0(1-\Delta\bar h)}};\\
\cos\gamma^-&=\frac{1}{(1-\Delta\bar h)\sqrt{1+\frac{2\Delta\bar h}{u_0(1-\Delta\bar h)}}};\\
\sin\gamma^-&=\pm\sqrt{\frac{\Delta\bar h}{1-\Delta\bar h}\cdot\frac{2(1-u_0)-\Delta\bar h(2-u_0)}{u_0+\Delta\bar h(2-u_0)}};
\end{aligned} \tag{21}$$

$$\begin{aligned}
\Psi_v^-&=A\frac{B(v^-)^2-1}{v^-};\quad \Psi_\gamma^-=A\,\mathrm{tg}\,\gamma^-;\\
\Psi_h^-&=A\frac{B-R^-}{(R^-)^2};\quad \Psi_m^-=C,
\end{aligned} \tag{22}$$

where $u_0=V_0^2R_0$, $\Delta\bar h=1-R^-/R_0$; A, B, C are the integration constants governed by the matching conditions; the subscript (0) refers to the trajectory apogee.

"Lower" region

$$\cos\gamma^+ = \cos\gamma_* + \left(\rho^+ - \rho_*\right)\frac{\mu K}{\beta},$$

$$v^+ = v_* \cdot \begin{cases} \exp\left\{\dfrac{\gamma_* - \gamma^+}{K}\right\}, & \text{as } K \neq 0 \\ \exp\left\{\dfrac{\rho^+ - \rho_*}{\beta \sin\gamma_*}\cdot\mu\right\}, & \text{as } K = 0 \end{cases} \tag{23}$$

$$\Psi_v^+ = q_{\max} K_v / v^+, \quad \Psi_h^+ = -\Phi K_h \beta \rho^+ / \rho_f;$$

$$\Psi_\gamma^+ = q_{\max} K_v \cdot \begin{cases} \left(1 - \dfrac{\sin\gamma^+}{\sin\gamma_f}\right)\dfrac{1}{K}, & \text{as } K \neq 0 \\ \left(1 - \dfrac{\rho^+}{\rho_f}\right)\dfrac{æ}{2}\operatorname{ctg}\gamma^+, & \text{as } K = 0 \end{cases} \tag{24}$$

$$\Psi_m^+ = q_{\max} K_h\left(1 - \rho^+/\rho_f\right), \quad æ = \frac{2K_h}{K_v},$$

where we have by virtue of (13)

$$\rho_f = -\frac{\beta æ}{2\mu}\sin\gamma_f, \tag{25}$$

and with due consideration of (23)

$$\sin\gamma_f = \begin{cases} \dfrac{\lambda}{1+\lambda^2}\left(\cos\chi - \sqrt{1+\lambda^2-\lambda^2\cos^2\chi}\right), & \text{as } K \neq 0 \\ \sin\gamma_*, & \text{as } K = 0 \end{cases} \tag{26}$$

$$\lambda = \frac{K_v}{K_h \cdot K}, \quad \cos\chi = \cos\gamma - \mu K\frac{\rho}{\beta}.$$

The constants A, B, and C in (22) are found from the conditions of matching the adjoint vector Ψ (transversality conditions). By virtue of (18) and (19) we obtain

$$h = h_*: \quad \Psi_v^- = \Psi_v^+ - \frac{2\xi}{\beta v_*}, \quad \Psi_\gamma^- = \Psi_\gamma^+,$$
$$\Psi_h^- = \Psi_h^+ + \xi,, \quad \Psi_m^- = \Psi_m^+ + \frac{\xi}{\beta}, \tag{27}$$
$$\left(\Psi^{\mathrm{T}} F\right)^+ = \left(\Psi^{\mathrm{T}} F\right)^-.$$

Hence [2,3]:

$$\xi = q_{\max}\cdot K_v \frac{1 + æ\rho_*/(\omega\rho_f) + \left(1 - v_*^2 R_*\right)D}{v_*^2 R_*^2(1+\omega)}$$

$$A = q_{\max} K_v D > 0,$$
$$B = \frac{1 + v_*^2 R_*\omega + \left(1 - æ\rho_*/\rho_f\right)/\mathrm{D}}{v_*^2(1+\omega)} > 1, \tag{28}$$
$$C = q_{\max} k\left[1 + \omega\frac{1 - æ\rho_*/\rho_f + \left(1 - v_*^2 R_*\right)D}{æ(1+\omega)}\right] > q_{\max} K_h,$$

where $D = \begin{cases} \operatorname{ctg}\gamma_*\left(1 - \sin\gamma_*/\sin\gamma_f\right)/K, & \text{as } K \neq 0, \\ \operatorname{ctg}^2\gamma_*\left(1 - \rho_*/\rho_f\right)æ/2, & \text{as } K = 0, \end{cases}$

$$\omega = \frac{2}{\beta v_*^2 R_*^2}.$$

Note that unlike the papers [6-9] we did not make assumptions concerning smallness of ω. Although $\omega \sim 1/\beta$, where $\beta \approx 900$ (for Earth), but $v^2 R < 1$ in the range of subcircular velocities under study and the condition $\omega \ll 1$ looks, at first glance, as an additional limitation. Let us show that in fact this condition stems naturally from the hypothesis of Allen-Eggers. Really, the condition (13) implying the termination of the trajectory for the full system (1) takes the form:

$$\rho_f = -\frac{\beta æ}{2\mu}\sin\gamma_f \cdot \left(1 + \frac{2}{æ\beta v_f^2 R_f^2}\right).$$

Comparison with the similar condition (25) within the framework of the hypothesis of Allen-Eggers for the lower region reveals that they coincide only when

$$\frac{2}{æ\beta v_f^2 R_f^2} \ll 1. \tag{29}$$

However, for the class of functionals under study (see (4) and (5)) $\dfrac{1}{æ} = \dfrac{K_v}{2K_h} \geq 1$, we have in the lower region that

$$\frac{d\left(v^+ R^+\right)}{dt} = -\mu\rho v^2 R + v^2\sin\gamma < 0,$$

$$\text{i.e.,} \quad \frac{1}{v_f^2 R_f^2} > \frac{1}{v_*^2 R_*^2}.$$

Thus, it follows immediately from (29) that

$$\omega \ll 1. \tag{30}$$

Thus, we have proved that the condition (30), which sets a lower bound on the range of velocities and altitudes under study, follows from the assumption on the capability of representing the reentry trajectory in the form of two matched sections.

From "equiaccuracy" considerations of the above-outlined formulas the condition (30) should be taken into account to simplify the formulas (28).

Altitude $h*$ of region matching

The formulas (21) to (28) allows one to determine explicitly the state trajectory based on the initial conditions, as well as the functional and adjoint variables as the functions of a current state vector, provided it is possible to find explicitly the altitude h_* from the condition (18). By considering (21), this condition can be written in the form of a nonlinear equation with respect to h_* or as a recurrent relation:

$$h_*^{(k)} = -\frac{1}{\beta}\ln\frac{h_*}{\mu\sqrt{1+K^2}v_0^2\left[1+\dfrac{2\left(h_0-h_*^{(k-1)}\right)}{v_0^2\left(1+h_*^{(k-1)}\right)\left(1+h_0\right)}\right]}, \quad (31)$$

where $h_*^{(0)} = h_0$.

From this it is easy to obtain

$$\delta h_*^{(k)} = -\omega\,\delta h_*^{(k-1)}.$$

Hence, corrections to h_* in each iteration are alternative to diminish very fast in geometric progression with a denominator of $(-\omega)$. By this is meant that in view of the condition (30) it is necessary, remaining within the framework of the hypothesis accepted at the beginning of the article, to confine the consideration only to the first iteration

$$h_* = -\frac{1}{\beta}\ln\frac{n_*}{\mu\sqrt{1+K^2}\cdot v_0^2}, \quad (32)$$

which yields the value of h_* with a relative error of no more than ω.

Accuracy analysis for analytical solutions

The approximate analytical solutions of the state and adjoint systems (21) to (28) are compared with the results of numerical integration of the sets (1) and (12) when $c_L = \text{const}$, $c_D = \text{const}$ and $P = 0$ in the subcircular range of initial velocities $v_0 < 1$. Fig. 2 shows the state trajectories. Respective adjoint functions are given in Fig. 3. It is seen that the analytical formulas yield a qualitatively correct description of variations in the state and adjoint variables for the complete range of initial velocities.

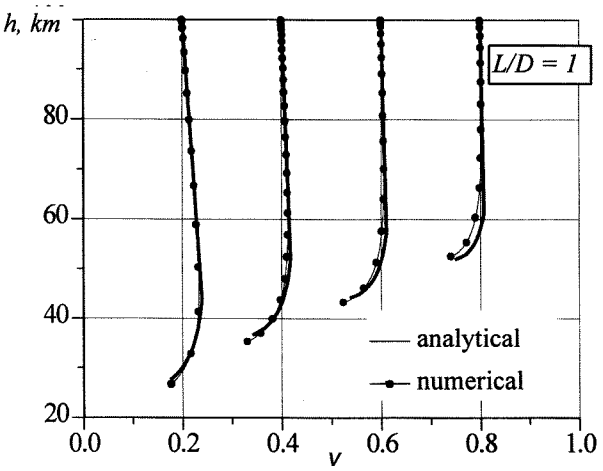

Fig. 2. Reentry trajectories for different initial velocities, $q=\rho v^2$, μ=6000, h_O=100km.

The most discrepancy between the analytical and numerical estimates is noted for Ψ_m (Fig. 3), which is accounted for, however, by an absolute smallness of this variable comparable with ω, i.e., of the quantity that was neglected when applying to the approximate motion model (see (30)).

The adjoint variables in (22), (28) and (24) are in proportion to q_{max} and the basic error of the formulas (22) and (24) is caused by the error of the analytical estimate of q_{max}. It is possible to refine the estimate of q_{max} within the framework of the approximate model under consideration by trying to "adjust" formally some parameters of the model to achieve the coincidence of the functionals in the numerical and analytical solutions.

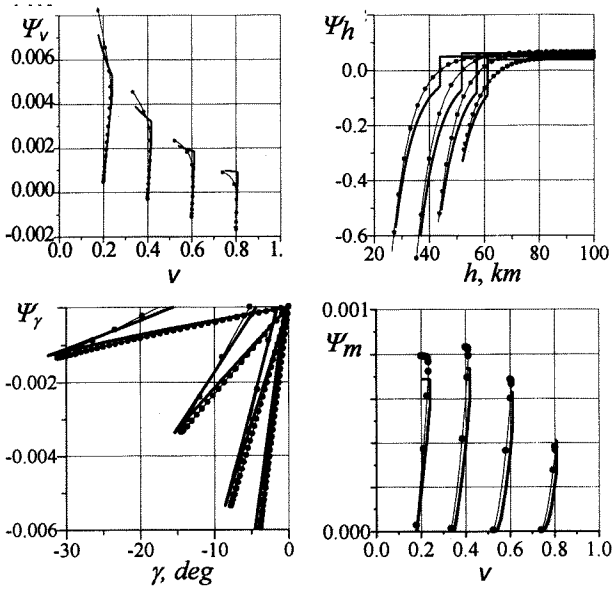

Fig. 3. A comparison of analytical (——) and numerical (—•—) adjoint functions $\psi_x = \dfrac{\partial q_{max}}{\partial x}$ for different initial velocities; $q=\rho v^2$, μ=6000, h_O=100km.

The conditional overload n_* at the point of matching the upper and the lower regions can serve as one of such parameters. It follows from (27), (28), and (31) that the influence of n_* on the functional is given by the relation

$$\frac{\delta q_{max}}{q_{max}} = \frac{\xi\delta h_*}{q_{max}} \cong W_n\frac{\delta n_*}{n_*}, \quad \text{where } W_n \sim \omega.$$

Thus, in view of (30) it may be inferred that the analytical solutions are not sensitive to small variations of n_*. Nevertheless, a substantial deviation in n_* enables the compensation for the analytical estimate error for q_{max}. The compensating values of the formal parameter n_* are shown in Fig.4 .

4. Optimal control

The optimality conditions for aerodynamic control in the "upper" region coincide with (16) because the aerodynamic forces do not enter the equations for the "upper" region and they can be considered only as disturbances. In the "lower" region, the aerodynamic force coefficients are taken to be constant, therefore, the conditions (16) are

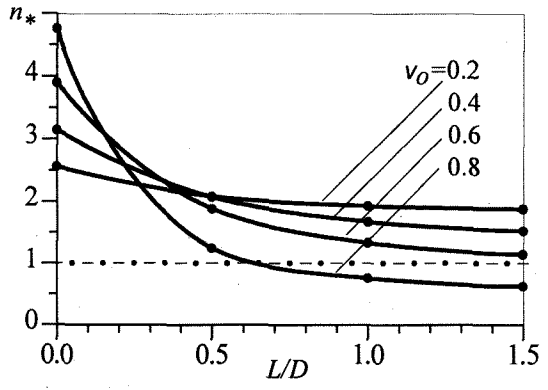

Fig. 4. The matching-point overload n_* for the coincidence of the analytical and numerical functional estimates; $q=\rho v^2$, μ=6000, h_O=100km.

satisfied in the "lower" region if Ψ_v^+ and Ψ_γ^+ are of constant signs. Let us prove that such is the case. Really, by virtue of (1), (12), and (24),

$$\frac{d\Psi_\gamma^+}{dt} = -v\cos\gamma\Psi_h^+ = \Phi k\beta v\cos\gamma\frac{\rho}{\rho_f} > 0$$

and, according to (14), $\Psi_{\gamma f}^+ = 0$. Hence, in the lower region $t \in (t_*, t_f)$ we have $\Psi_\gamma^+ < 0$. From (24) it follows $\Psi_v^+ > 0$.

Thus, the optimality conditions for aerodynamic control in the "upper" and "lower" regions are governed by the same conditions (16).

The optimality conditions for thrust angle-of-attack (see (16)) are valid for an approximate motion model only when thrust-caused reentry trajectory disturbances are small.

Substituting the integrals (21) to (28) in (16) gives (3) (Fig. 5):

$$c_{D\text{opt}} = \begin{cases} c_{D\max}, & v > 1/\sqrt{B} \text{ or } h < h_* \\ c_{D\min}, & v < 1/\sqrt{B} \text{ and } h > h_* \end{cases}$$

$$c_{L\text{opt}} = \begin{cases} c_{L\max}, & \gamma < 0 \\ c_{L\min}, & \gamma > 0 \end{cases}$$

$$\varphi_{\text{opt}}^+ = \begin{cases} \pi + \operatorname{arctg}\left(1 - \dfrac{\sin\gamma^+}{\sin\gamma_f}\right)\dfrac{1}{K}, & \text{as } K \neq 0 \\ \pi + \operatorname{arctg}\left(\dfrac{æ}{2}\operatorname{ctg}\gamma^+\left(1 - \dfrac{\rho^+}{\rho_f}\right)\right), & \text{as } K = 0 \end{cases} \quad (33)$$

$$\varphi_{\text{opt}}^- = \begin{cases} \operatorname{arctg}\dfrac{\operatorname{tg}\gamma^-}{Bv^2 - 1}, & \text{as } v < 1/\sqrt{B} \\ \operatorname{arctg}\dfrac{\operatorname{tg}\gamma^-}{Bv^2 - 1} - \pi\operatorname{sign}\gamma^-, & \text{as } v > 1/\sqrt{B} \end{cases}$$

As is obvious from (33) and Fig. 5, there are two types of optimal control laws. The type II differs qualitatively from the type I by the presence of a region in the vicinity of the apogee in which the vehicle should accelerates but not decelerates in order to reduce maximum reentry loads.

Since $v^- \geq v_0$, therefore the excess of the velocity at apogee v_0 over a critical value v_{crit} proves to be, according to (33), the indication of appearing such a region. The conditions for existence of a certain type of optimal control laws are following:

the type I - $\psi_{v0} > 0$,

the type II - $\psi_{v0} < 0$,

where ψ_{v0} is the velocity-adjoint variable at apogee.

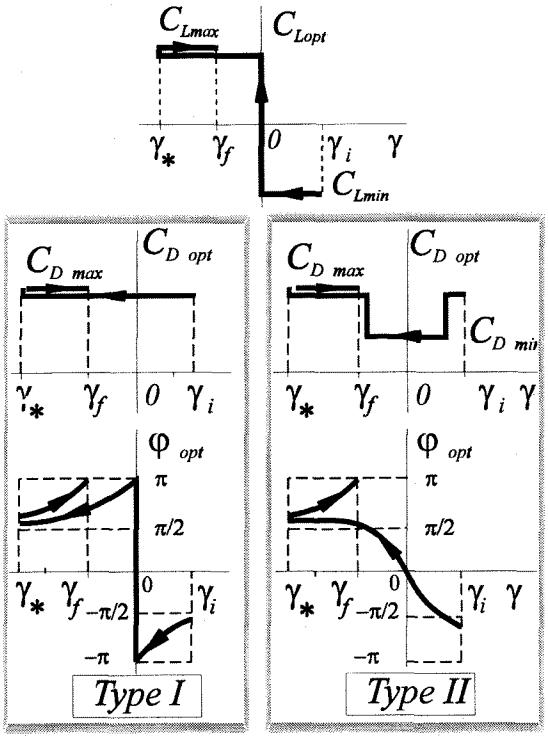

Fig. 5. Structures of the optimal controls laws.

The critical velocity is found from the equation

$$v_{crit.} = v_0(h_0, K): \quad 0 = \psi_{v0} \cong \frac{v_0^2 B(v_0, h_0, K) - 1}{v_0}. \quad (34)$$

It can be shown that for a high velocity

$$\frac{\partial v_{\text{crit}}}{\partial K} < 0, \quad (35)$$

therefore, the highest critical velocity corresponds to ballistic vehicles with $K = 0$. At $K = 0$, we obtain from (22), (23), (25), (26), (28), and (34) that

$$u_0 = v_{\text{crit}}^2 \cdot R_0 = \frac{1 + \bar{\beta}\Delta\bar{h}(1 - \Delta\bar{h})\left[1 - \dfrac{2}{æ}(1 - \Delta\bar{h})^2(1 + \varepsilon)\right]}{(1 - \Delta\bar{h})\left[1 - \dfrac{2}{æ}\bar{\beta}\Delta\bar{h}(1 - \Delta\bar{h})\left(1 - \dfrac{\Delta\bar{h}}{2}\right)(1 + \varepsilon)\right]}, \quad (36)$$

where $\varepsilon = (1 - æ)\dfrac{\rho_*/\rho_f}{1 - \rho_*/\rho_f}$, $\bar{\beta} = \beta R_0$, $\sqrt{u_0}$ is the critical velocity at apogee related to the local circular velocity v_c.

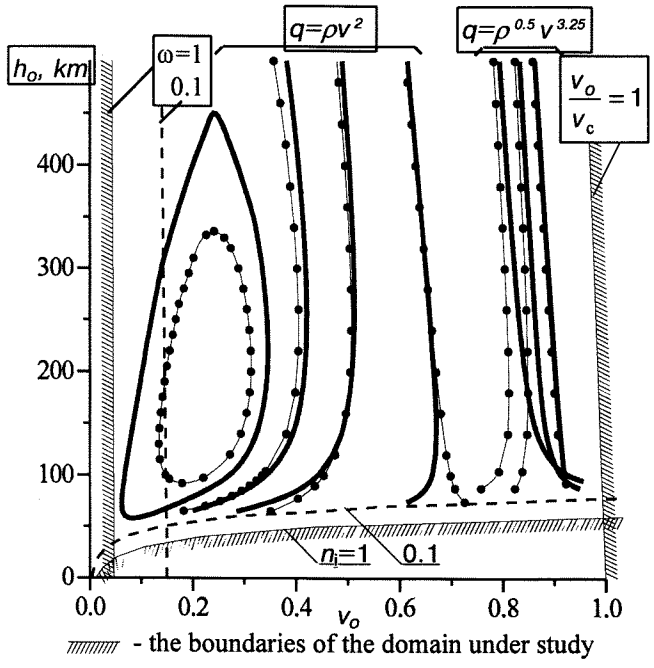

Fig. 6. A comparison of the analytical (——) and numerical (—•—) calculations of the critical velocities $v_o=v_{crit.}$ for different apogee altitude h_o, L/D-ratio and functional type.

If the functional is a maximum dynamic pressure (overload) then $æ = 0$ and $\varepsilon = 0$. Thus, it follows from (36) that

$$u_0 \le \max_{\Delta\bar{h}} \max_{K} u_0(K,\Delta\bar{h}) = u_0(0,\delta) = \\ = \frac{1-\delta}{2-\delta} \le \max_{\delta} u_0(0,\delta) = \frac{1}{2},$$

where $\delta = \sqrt{\frac{5}{\beta}}$ is a small value ($\delta \le 0.075$ for Earth).

Hence, if functional $\Phi = \max_t \rho v^2$ then

$$\sqrt{u_0} = \frac{v_{crit}}{v_c} \le \frac{1}{\sqrt{2}}. \qquad (37)$$

In this case, the limit case $u_0 = \frac{1}{2}$ corresponds to the reentry of a ballistic vehicle into an atmosphere with an infinitely great parameter β.

If the functional is a maximum heating rate (see (5)), it is possible to derive the estimate

$$u_0 \le \max_{K,\Delta\bar{h},\beta} u_0 \cong 1 - \frac{æ}{2} \qquad (38)$$

from (36) with an accuracy up to terms ~ ε.
In the case corresponding to (6), it follows from (38) that

$$\max v_{crit}/v_c \approx 0.92 \qquad (\text{for } \Phi = \max_t \rho^{0.5} v^{3.25}), \qquad (39)$$

i.e., the type II of optimal control laws is realized for nearcircular initial velocities.

In general case, the type I of the optimal control laws is realizede in a domain

$$v_{crit.\,min}(h_0, K=fix) < v_0 < v_{crit.\,max}(h_0, K=fix), \qquad (40)$$

where the boundaries $v_{crit.\,min}$ and $v_{crit.\,max}$ are two branches of the critical velocity dependence (34) on the apogee altitude h_0 and correspond to two solutions of the equation (34), if the solutions exist for the used L/D-ratio.

The typeII is optimal outside the domain (40).

The analytical estimations of the domains (40) are in line with the numerical integration results (Fig. 6) even in a vicinity of the validity limit due to the condition (30).

Fig. 7 shows the domains (40) for functionals (3),(4) and (3),(6) in details. The left boundary $v_{crit.\,min}$ for functional (3), (6) (the heating rate) is not shown because it lies outside the velocity range under consideration (see Fig. 6) and corresponds to a vicinity of zero. When the functional is the maximum dynamic pressure the type I of the optimal control laws exists only for vehicles with $K = L/D < 1.8$. At $L/D > 1.8$, the type II is optimum for every initial condition $\{v_0, h_0\}$ under study.

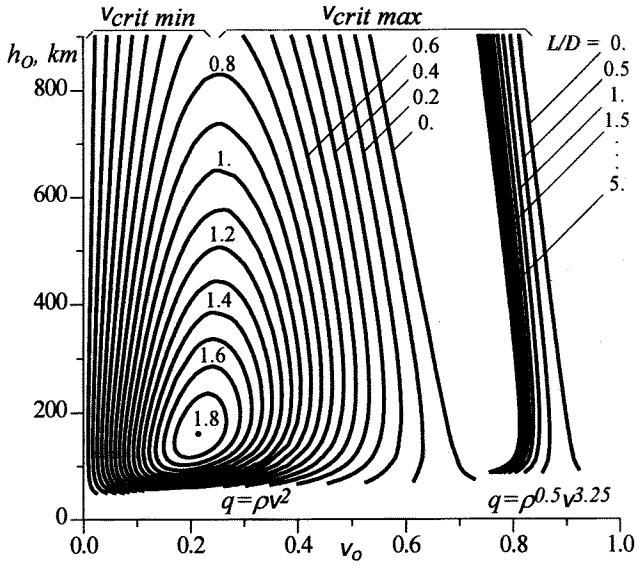

Fig. 7. Critical initial regimes with respect to the maximum dynamic pressure and to the maximum heating rate (numerical integration results); μ=6000.

Effectiveness of control

The analytical expressions (22) and (24) for the adjoint variables allow the effectiveness of reducing maximum loads due to small control actions to be estimated using the Bliss's formula [12] for a variation of the functional

$$\delta\Phi = \Psi^T \delta x|_{t_f} = \Psi^T \delta x|_t + \int_t^{t_f} \Psi^T \delta_u F dt, \qquad (41)$$

where $\delta_u F$ is the variation of right-hand sides of equations of motion due to a control variation. By small control actions are meant here control variations which exert a quasilinear integral influence on the functional. In particular, finite increments of the control parameters (c_D, c_L, P) during a small time interval ("needle" variations) can be considered small.

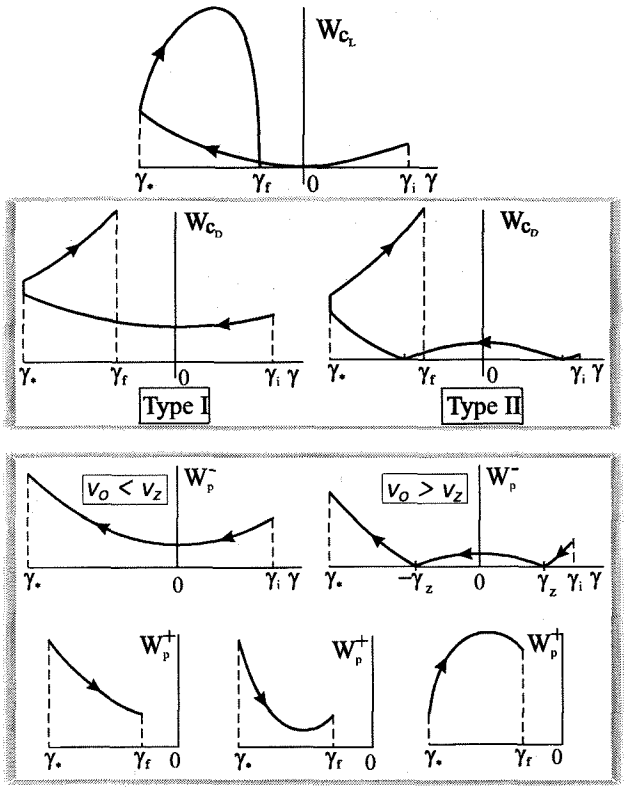

Fig. 8. The effectiveness of the small optimal control actions on the reentry trajectory.

According to (41), the relative effectiveness of a local optimal variation in the effective lift coefficient for the set (1) is given by the quantity

$$W_{c_L} = -\frac{\delta\bar{\Phi}}{\delta c_L / c_D\,\delta t} = \mu\rho v \frac{|\Psi_\gamma|}{\Phi}, \quad \delta\bar{\Phi} = \delta\Phi/\Phi. \qquad (42)$$

It follows from the integrals (21) to (24) and (42) that W_{c_L} increases monotonically with the dynamic pressure except for some vicinity of the final point x_f at which $W_{c_L} = 0$ by virtue of the transversality conditions (14) (Fig. 8).

Similarly to (42), the relative effectiveness of a local optimal variation in the aerodynamic drag coefficient is defined as follows:

$$W_{c_D} = -\frac{\delta\bar{\Phi}}{\delta c_D / c_D\,\delta t} = \mu\rho v^2 \frac{|\Psi_v|}{\Phi}.$$

According to (21) to (24) W_{c_D}, increases monotonically with the dynamic pressure excluding, probably, the vicinity of the apogee where there is a local maximum W_{c_D} at the apogee velocity v_0 such that the type II of the controls laws is optimum. It should be taken into account that in the latter case some reduction in the functional $q_{\max}$ is attained when the coefficient c_D decreases in the vicinity of the apogee (see (33) and Fig. 5).

Let us define the effectiveness of a local optimal start of engines as

$$W_P = -\frac{\delta\bar{\Phi}}{\delta v_{\text{char}}} = \frac{1}{\Phi}\left(\sqrt{\Psi_v^2 + \left(\frac{\Psi_\gamma}{v}\right)^2} + \frac{\Psi_m}{c}\right), \qquad (43)$$

where $\delta v_{\text{char}} = P\delta t$ is the variation of the dimensionless characteristic velocity of the propulsion system. The analysis of the derivative

$$\dot{W}_P^- = -\frac{A^2}{\Phi}\frac{\operatorname{tg}\gamma}{v_0 R_0}\frac{z}{\sqrt{\Psi_v^2 + \left(\frac{\Psi_\gamma}{v}\right)^2}}, \text{ where } z = \frac{B^2 v_0^2 R_0^2}{R^3} - 1,$$

reveals that the function $W_P^-(\gamma)$ can be of two types (see Fig.8): at $v_0 < v_z$, W_P^- has one minimum at the apogee, while at $v_0 > v_z$, there are two zero minima of W_P^- at $\gamma = \pm\gamma_z$, $0 < \gamma_z < |\gamma_*|$, and a local maximum at the apogee. Under assumption that $\Delta\bar{h}$ is a small value it is possible to obtain that

$$1 > v_z\sqrt{R_0} > 1 - 2\Delta\bar{h},$$

i.e., the second type of the function W_P^- can exist only at near circular velocities.

The analysis of the derivative $\dot{W}_P^+$ for the lower region gives that when the inequalities

$$|\operatorname{tg}\gamma_*| \le \left(K + \frac{2(2-æ)}{Kæ^2}\right)\left(1 + \frac{2}{\sqrt{4+K^2æ^2}}\right); (K \ne 0) \qquad (44)$$

and $v_f > c$

are satisfied we have $\dot{W}_P^+ < 0$ and a maximum effectiveness of employing engines is achieved at the moment of entering the dense atmospheric layers ($h = h_*$). The conditions (44) for ballistic vehicles ($K = 0$) are satisfied a fortiori at $v_0 > ce^{æ/2}$. If the conditions (44) are violated, for example, when reentering at small velocities, the best moments of employing engines to reduce maximum loads can be within the lower region (see Fig. 8).

5. Influence of initial conditions

The upper section is a Keplerian trajectory, therefore initial conditions are governed by two parameters, for example, by the altitude h_0 and the velocity v_0 at apogee.

By virtue of (15), the influence of $\{v_0, h_0\}$ on the functional $q_{\max}$ is described by the functions

$$\frac{\partial q_{\max}}{\partial v_0} = \Psi_{v_0} \cong A\frac{Bv_0^2 - 1}{v_0}, \qquad \frac{\partial q_{\max}}{\partial h_0} = \Psi_{h_0} \cong A\frac{B - R_0}{R_0^2}. \qquad (45)$$

Fig. 9 shows the behavior of the influence functions Ψ_{v_0} which are obtained from the approximate formulas (22) and (28) and by numerical integration of the sets (1) and (12). The disagreement is caused primarily by the error of the analytical definition of q_{max}.

As follows from (45), the initial velocity v_0, at which the local extremum load is attained when reentering, coincides with the critical velocity v_{crit} (34) governing the change of the optimal control structure. The left branch $v_{crit.\ min}(h_0)$ of the curve $v_{crit.} = v_0(h_0)$ consists of local minima of the function $q_{max}(v_0)$ (Fig. 10). The right branch $v_{crit.max}(h_0)$ is a set of local maxima of the function $q_{max}(v_0)$, i.e., the most dangerous initial velocity v_0 in terms of loads acting during the reentry. Fig. 7 presents values of the critical velocity v_0 for different initial altitudes h_0 and L/D-ratios. The results obtained using the approximate formulas and by numerical integration (Fig. 6) are in a rather good agreement between each other and with the estimate (37) and (39).

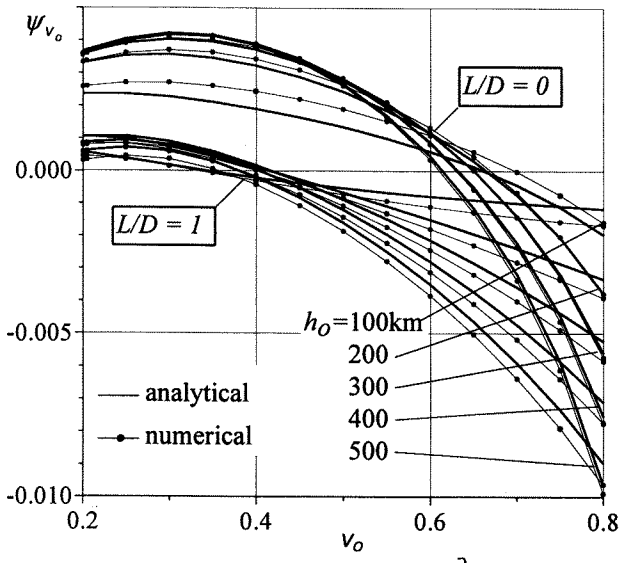

Fig. 9. Velocity-adjoint variable $\psi_{v_o} = \frac{\partial q_{max}}{\partial v_o}$ at apogee as a function of the speed v_o and altitude h_o at apogee for ballistic and lift vehicles; $q=\rho v^2$, μ=6000.

Earth rotation effect

The Earth rotation effect can be reduced only to an alteration in matching conditions for the state system at the altitude h_*. To do this, let us assume that in the upper region Eqs. (1) describe the motion in the inertial coordinate system, while in the lower region they represent the motion in the noninertial coordinate system fixed to the rotating Earth.

Let the jump conditions

$$v_*^+ = v_*^- + \delta v_*; \quad \gamma_*^+ = \gamma_*^- + \delta\gamma_*$$

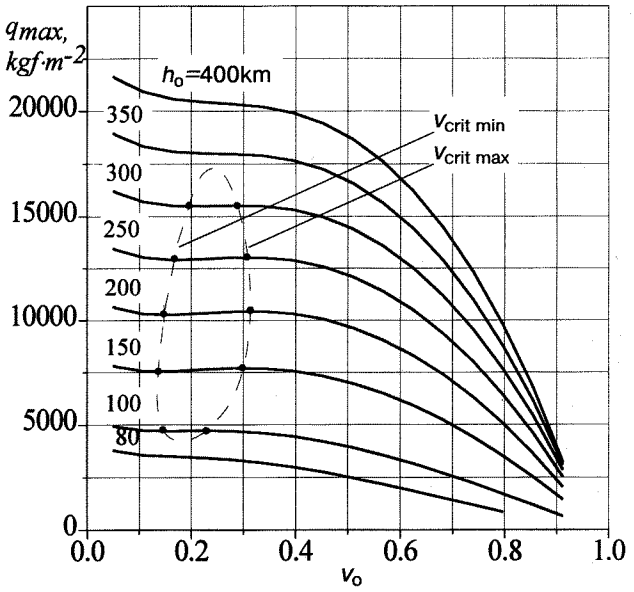

Fig. 10. The functional $q_{max} = \max_{\{t\}} \rho v^2$ as a function of the apogee velocity v_o for different apogee altitude h_o; $L/D = 1.5$.

be satisfied at the point of region matching in transiting from the inertial coordinates to the noninertial ones. Because the vertical velocity component in this transition does not change

$$\delta(v_* \sin\gamma_*) = 0,$$

variations of δv_* and $\delta\gamma_*$ are interrelated:

$$\delta\gamma_* = -\operatorname{tg}\gamma_* \frac{\delta v_*}{v_*}.$$

Assuming that the matching altitude h_* remains unchanged it is possible to find a variation of the functional from (41) with due consideration of the Earth rotation:

$$\delta\Phi = \Psi_{v_*}^+ \delta v_* + \Psi_{\gamma_*}^+ \delta\gamma_* = \begin{cases} \Phi K_v \left[1 - \left(1 - \frac{\sin\gamma_*}{\sin\gamma_f}\right)\frac{\operatorname{tg}\gamma_*}{K}\right]\delta\bar{v}_*, & \text{as } K \neq 0 \\ \Phi\left[K_v - K_h + K_h \frac{\rho_*}{\rho_f}\right]\delta\bar{v}_*, & \text{as } K = 0 \end{cases}$$

where $\delta\bar{v}_* = \delta v_*/v_*$.

Since $n_* = \mu\rho_* v_*^2 \ll \mu\rho_f v_f^2 = n_f$, then $\rho_* v_f^2 < \rho_* v_*^2 \ll \rho_f v_f^2$ and, hence, $\rho_* \ll \rho_f$.

Thus, at $K = 0$ we have

$$\delta\bar{\Phi} \cong (K_v - K_h)\delta\bar{v}_*. \qquad (46)$$

If $K \neq 0$, then, assuming that $\sin\gamma_f \approx \gamma_f$; $\cos\gamma_* \approx 1 - \gamma_*^2/2$, we obtain

$$\delta\bar{\Phi} = K_v\left(1 - æ - \frac{\gamma_*}{K}\right)\delta\bar{v}_*. \qquad (47)$$

If the functional Φ is a maximum dynamic pressure ($æ = 1$) the estimates (46) and (47) take the form:

$$\delta\bar{\Phi} = \begin{cases} -\gamma_* \dfrac{K_v}{K}\delta\bar{v}_*, & K \neq 0 \\ \delta\bar{v}_*, & K = 0 \end{cases}$$

where $\delta\bar{v}_*$ is the relative velocity increment at the moment of entering the dense atmospheric layers due to the Earth rotation.

Effect of variations of atmospheric parameters and aerodynamic characteristics

Real dependencies of the aerodynamic characteristics on flight regimes ($\tilde{c}_D(h.v), \tilde{c}_L(h,v)$) and the parameter β on the altitude h: $\tilde{\beta}(h)$ can be taken into account in the first approximation within the framework of the accepted model (20). To accomplish this, averaged values of these parameters ($\bar{c}_D, \bar{c}_L, \bar{\beta}$) should be used as constants (20). The averaged values will be found from the condition of coinciding the functional for real and averaged parameter values. Variations in the functional for varying parameters (20) will be estimated within the first variation of (41). Then, using the integrals for the state and adjoint systems in the lower region (23) and (24) we obtain

$$\bar{c}_D = \frac{\int_{v_*}^{v_f} \tilde{c}_D\left(h(v),v\right)\frac{dv}{v}}{\ln(v_f/v_*)}, \quad \bar{c}_L = \frac{\int_{\gamma_*}^{\gamma_f}\left(1 - \frac{\sin\gamma}{\sin\gamma_f}\right)\tilde{c}_L\left(h(\gamma),v(\gamma)\right)d\gamma}{K\left(\ln(v_*/v_f) - K_h/K_v\right)}$$

$$\bar{\beta} = -\frac{\beta}{\rho_f}\frac{\int_{h_*}^{h_f}\rho h\tilde{\beta}(h)dh}{h_*\rho_*/\rho_f - h_f + (\rho_*/\rho_f - 1)/\beta} \approx -\frac{\beta}{\rho_f h_f}\int_{h_*}^{h_f}\rho h\tilde{\beta}(h)dh \quad (\text{if } \beta h_f \gg 1)$$

The state variables under the integrals are taken for the nominal trajectory with parameters (20).

Applications

The theoretical investigation results concerning non-equilibrium atmospheric reentry are applied to solving a number of practical problems mentioned in Introduction. Various means and techniques of reducing maximum overloads in entering the dense atmospheric layers are compared when solving the problem of returning spent components of space transport systems with the employment of the analytical estimates of the optimal control effectiveness, the solutions of the adjoint system and the functions of the initial state vector influence on the functional. Among them, the capabilities of stabilizing vehicles at optimal angles of attack, of using brake flaps and parachute systems in optimal regime, as well as of optimizing separation conditions are analyzed.

A complex investigation of the problems regarding recovery of the orbiter and the crew for different kinds of space transport systems as a result of emergency orbital insertion abort is carried out. Three types of techniques are considered. The first type implies the control optimization by applying standard means available in the orbiter (brake systems, roll and angle-of-attack control, orbital maneuvering engines etc.). The second type suggests the application of special auxiliary means (for example, emergence recovery system engines intended in the schedule flight only for emergence sideways deflection of the spacecraft from the start position). As for the third type, it presumes optimal variations in the initial conditions of emergency reentry. Because the initial conditions of emergency reentry correspond to the ascent conditions according to the schedule program, an admissible range of the trajectory parameter values is identified starting with which the orbiter can reentry without exceeding permissible loads. It is suggested that the above-outlined limitations on the suborbital portion of the schedule ascent trajectory stemming from the requirements for fail-safety should be called "the ascent corridor"[15] by analogy with an "entry corridor" in the problem of reentry with supercircular velocities[4,5].

In all the listed problems, the application of the analytical solutions for the adjoint variables and the functional with taking account of corrections for real characteristics of the atmosphere and the vehicle ensures an adequate accuracy.

Conclusions

The problem of minimizing maximum dynamic pressure (overloads) and heating rate is investigated for non-equilibrium entering the dense atmospheric layers with initial velocities which are significantly lower than the local circular velocity. It is shown that direct matching of analytical solutions for the state and adjoint equations being valid under conditions of the Keplerian motion on the initial trajectory section and the Allen-Eggers hypothesis on the final coasting trajectory section in the dense atmospheric layers makes it possible to investigate with a high accuracy the optimal control laws, their effectiveness and the influence of the vehicle characteristics and initial conditions on the functional.

It is established that the optimal control laws with the application of the aerodynamic drag coefficient and the thrust vector can be of two types. The first type proves to provide the vehicle deceleration within the whole reentry trajectory. As for the second type, it ensures the vehicle deceleration only on the trajectory portions lying below a certain altitude. At higher altitudes up to the apogee, the minimization of peak loads is achieved due to the vehicle acceleration. The physical meaning of the boundary separating the optimality regions of these control laws in the plane of apogee velocity V_0 -apogee altitude h_0 is in the fact that it corresponds to critical velocities $V_o = V_{crit}(h)$ at

which the loads are extreme in the regime of entering the dense atmospheric layers.

It is proved that the critical velocity rises as the vehicle L/D-ratio decreases. If the functional to be minimized is a maximum heating rate the critical velocity is within the near circular range.

If the functional to be minimized is a maximum overload then v_{crit} is not more than $1/\sqrt{2}$ of the local circular velocity. For vehicles with $L/D = 0$, the second type of the optimal control structure is realized when the velocity at apogee is $v_o > v_{crit} \approx 1/\sqrt{2}$. If $1.8 > L/D > 0$, the dependencies $V_o = V_{crit}(h_o)$ describe closed curves bounding simple connected domains inside of which the first type of the control laws is optimal, and outside the second type. On further increasing when $L/D > 1.8$, the optimality region for the first type of the control laws becomes degenerate and, accordingly, the second type proves to be optimal within the whole range of subcircular velocities under consideration, a maximum overload diminishing monotonically as the initial velocity V_o at apogee increases.

The approximate analytical relations cited above can be applied to solve practical problems as concerns the safe atmospheric reentry of spent components of space transport systems, vehicles performing test suborbital flights, recoverable vehicles because of orbital ascent abort etc. For these purposes, real aerodynamic characteristics, the dependence of the atmospheric density on altitude, the Earth rotation effect etc. can be taken into account rather accurately within the approximate trajectory model under consideration by means of a special choice of parameters of this model based on the analysis of the first variation of the functional and the influence functions.

References

1. Filatyev, A.S., "Reduction of Maximum Dynamic and Heat Loads in Passive Motion of Hypersonic Vehicles Using Small Control Actions," Uchenye Zapiski TsAGI, v. 9, No. 2, 1978.
2. Filatyev, A.S., "Approximate Analytical Synthesis of the Optimal Control of Hypersonic Vehicles in Atmospheric Motion with Subcircular Velocities," Uchenye Zapiski TsAGI, v. 11, No.1, 2 , 1980.
3. Filatyev, A.S., "Space Vehicle Safety Problem: Reentry with Subcircular Speeds," IAA 6.1-93-731, 44th Congress of the IAF, October 16-22, 1993/ Graz, Austria.
4. Yaroshevsky, V.A., "Spacecraft Reentry into the Atmosphere," Nauka Publisher, Moscow, 1988.
5. Vinh, N.X., Busemann, A., Culp, R.D., "Hypersonic and Planetary Entry Flight Mechanics," The University of Michigan Press, 1980.
6. Willes, R.E., Fransisco, M.C., Reid, J.G., and Lim, K.W., "An Application of Matched Asymptotic Expansions to Hypervelocity Flight Mechanics," AIAA Paper 67-598, 1967.
7. Shi, Y.-Y., and Pottsepp, L., "Asymptotic Expansion of a Hypervelocity Atmospheric Entry Problem," AIAA Journal, N2, 1969.
8. Shi, Y.-Y., "Matched Asymptotic Solutions for Optimum Lift Controlled Atmospheric Entry," AIAA J., N 11, 1971.
9. Frostic, F., and Vinh, N.X., "Optimal Aerodynamic Control by Matched Asymptotic Expansions," Acta Astronautica, v. 3, pp. 319-332.
10. Allen, H.J., and Eggers, A.J., "A Study of the Motion and Aerodynamic Heating of Missile Entering the Earth Atmosphere at High Supersonic Speed," NASA Rep. N 1381, 1958.
11. Lawden, D.F., "Optimal Trajectories for Space Navigation," London, 1963.
12. Bliss, G.A., "Mathematics for Exterior Ballistics," N.Y. 1944.
13. Filatyev, A.S., "Optimization of Spacecraft Ascent Using Aerodynamic Forces," IAF-92-0022, 43rd IAF Congress, Aug. 28 - Sep. 5, 1992, Washington, USA.
14. Kemp, N., Riddell, F., "Heat Transfer to Satellite Vehicles Reentry Atmosphere," Jet Propulsion, v.21, No. 2, 1957.
15. Pontryagin, L.S., Boltyansky, V.G., Gamkrelidze, R.V., and Mishchenko, Ye.F., "The Mathematical Theory of Optimal Processes," Nauka Publisher, Moscow, 1972.
16. Filatyev, A.S., and Yanova, O.V., "The Optimization of Ascent Trajectories with Continuum of Branches," IAF-94-A.2.019, 45th IAF Congress, October 9-14, 1994, Jerusalem, Israel.